

## Optical identification of ROSAT-FSC sources<sup>★</sup>

A. M. Mickaelian<sup>1</sup>, L. R. Hovhannisyanyan<sup>1</sup>, D. Engels<sup>2</sup>, H.-J. Hagen<sup>2</sup>, and W. Voges<sup>3</sup>

<sup>1</sup> Byurakan Astrophysical Observatory and Isaac Newton Institute of Chile, Armenian branch, Byurakan 378433, Aragatzotn province, Armenia

e-mail: aregmick@apaven.am; lili\_hov@rambler.ru

<sup>2</sup> Hamburger Sternwarte, Gojenbergsweg 112, 21029 Hamburg, Germany

e-mail: [dengels;hhagen]@hs.uni-hamburg.de

<sup>3</sup> Max-Planck-Institut für Extraterrestrische Physik, Postfach 1312, 85741 Garching, Germany

e-mail: whv@mpe-garching.mpg.de

Received 2 August 2005 / Accepted 7 November 2005

### ABSTRACT

The Byurakan/Hamburg/ROSAT Catalogue (BHRC) of the optical identifications of X-ray sources is presented. The BHRC includes all 2791 sources from the ROSAT-FSC with  $|b| \geq 30^\circ$ ,  $\delta \geq 0^\circ$  and ROSAT count rate  $CR > 0.04 \text{ cts s}^{-1}$ . For the optical identifications, we used the Hamburg Quasar Survey (HQS) digitized spectroscopic plates, the DSS1 and DSS2 (blue, red, and IR) images, the MAPS photometric data, the USNO-B1.0 (for proper motions), the NVSS and FIRST radio, and the IRAS and 2MASS infrared catalogues. From the DSS images we obtained positional, brightness, color, extension, variability, proper motion information, and measured the optical-to-X-ray distance. Based on the DSS images, a morphological classification was made. Available SIMBAD and NED data were used as well. Cross-correlations were made with AGN, white dwarf, and cataclysmic variable catalogues (322/8/7 associations, respectively). We managed to identify 97% of sources (2696 sources) that are associated with 3202 optical objects. 2248 X-ray sources have a single optical counterpart, 144 have a double or multiple optical counterpart (binaries, galaxy groups etc.), and 304 have ambiguous identifications. We find that some of the latest might actually be blends of two X-ray sources that were not resolved by ROSAT. The QSOs and AGN represent the largest group of X-ray counterparts (56.2%); bright stars (including late type stars, but excluding WDs and CVs) are counterparts for 33.2% of sources, and the bright galaxies and groups of galaxies comprise 9.2%. We found a number of close galaxy pairs (possibly interacting/merging galaxies) that are counterparts for X-ray sources (3.0%), as well as 1.0% WDs and 0.4% CVs. The BHRC may be used for selection and for studies of samples of various classes of X-ray emitters.

**Key words.** surveys – X-rays: general – X-rays: galaxies – X-rays: stars – X-rays: binaries – catalogs

### 1. Introduction

The ROSAT All-Sky Survey (RASS) is so far the only all-sky survey in X-rays (Trümper 1983). The energy range covered was from 0.07 to 2.4 keV. Two main ROSAT catalogues have been published: the ROSAT Bright Source Catalogue (BSC), containing 18 811 sources with count rates  $>0.05 \text{ cts s}^{-1}$  (Voges et al. 1999), and the ROSAT Faint Source Catalogue (FSC), containing 105 924 sources with count rates  $<0.05 \text{ cts s}^{-1}$  (Voges et al. 2000).

A number of projects on optical identification of these sources have been undertaken, including a few large ones. The ROSAT North Ecliptic Pole Survey (Henry et al. 2001; Voges et al. 2001) and the LSW-INAOE-MPE project

(Zickgraf et al. 1997; Appenzeller et al. 1998; Krautter et al. 1999) aimed to identify all ROSAT sources in given (small) regions without preselection of any X-ray data (count rates, hardness ratios, or source extension). The ROSAT Bright Survey (RBS) was a large area project, where ~2000 sources were identified with count rates  $>0.2 \text{ cts s}^{-1}$  (Fischer et al. 1998; Schwöpe et al. 2000). The largest work on optical identifications of the ROSAT sources so far is the Hamburg-RASS Catalogue (HRC) of Optical Identifications (Zickgraf et al. 2003), where 5341 BSC sources with  $\delta > 0^\circ$  and  $|b| > 30^\circ$  ( $10\,313 \text{ deg}^2$ ) were identified using the Hamburg Schmidt low-dispersion spectra (18% could not be identified). A search for bright optical counterparts ( $O < 16.5^m$ ) of X-ray sources of the ROSAT FSC was made by Véron-Cetty et al. (2004) by cross-correlating the FSC with the USNO-A2.0 (Monet et al. 1996) and with MAPS (Cabanela et al. 2003), and subsequent classification of the candidates with the low-dispersion HQS spectra. Their goal was to obtain a large, optically bright, X-ray

<sup>★</sup> Table 1 is only available in electronic form at the CDS via anonymous ftp to cdsarc.u-strasbg.fr (130.79.128.5) or via <http://cdsweb.u-strasbg.fr/cgi-bin/qcat?J/A+A/449/425>

selected AGN sample. Though many of the 3212 optical candidates were found to be chance associations, a few hundred real counterparts could be determined, from which 42 new AGNs have so far been discovered by follow-up observations.

Despite these efforts, the physical nature of only about 10% of all ROSAT sources is known at present, and new optical identifications are important for making possible follow-up studies of these sources. In the context of a Byurakan-Hamburg collaboration on studies of ROSAT sources (aimed mainly at AGNs), we have undertaken a project of optical identifications of ROSAT FSC sources in the same area as in the HRC to extend this project to sources with count rates  $\geq 0.04$  cts  $s^{-1}$ . In addition to the HQS low-dispersion spectra used in the HRC, we used DSS1 and DSS2 (blue, red, and IR) images in the corresponding X-ray fields and cross-correlated the candidate counterparts with all available catalogues to improve the identifications. We present here the Byurakan/Hamburg/ROSAT Catalogue (BHRC) of Optical Identifications. The BHRC Catalogue contains data for 3202 optical objects corresponding to 2696 X-ray sources.

## 2. The sample of ROSAT FSC sources

Our area of study was the same as in the HRC ( $\delta > 0^\circ$  and  $|b| > 30^\circ$ ). In this area, there are 16 446 ROSAT FSC sources with  $\geq 0.02$  cts  $s^{-1}$ , 6886 sources with  $\geq 0.03$  cts  $s^{-1}$ , and 2791 sources with  $\geq 0.04$  cts  $s^{-1}$ . To have a reasonable number of X-ray sources for identifications, we selected sources with  $\geq 0.04$  cts  $s^{-1}$ . This sample also includes 649 sources with  $\geq 0.05$  cts  $s^{-1}$ , which did not enter the ROSAT BSC, as less than 15 photons had been detected from each of them (the BSC selection criterion on the number of photons). The DSS1 red, DSS2 blue, red, and IR images have been retrieved for each of these 2791 X-ray sources to search for optical counterparts.

Of these sources 683 had been included in the identification program of Véron-Cetty et al. (2004). They have optical counterparts brighter than  $O = 16.5$  in USNO-A2.0. However, because of many chance associations among these counterparts (about half of them turned out to be FG stars), we decided to keep all these sources in the present project to find their genuine counterparts.

## 3. Identification technique

### 3.1. The HQS spectra and DSS images

The identification was performed in several steps. In the first step, the identification technique for the ROSAT sources was similar to the one in the HRC project (Bade et al. 1998; Zickgraf et al. 2003). However, we introduced some new criteria in addition and used more resources. First, the DSS1 (McGlynn et al. 1994) and DSS2 blue/red/IR (Lasker et al. 1996) direct images and the Hamburg Quasar Survey (HQS) low-dispersion spectra (Hagen et al. 1995) were inspected in the error circles of the X-ray sources. We used  $3\sigma$  error radii obtained from the  $1\sigma$  positional uncertainties given in the FSC for each source. Figure 1 gives the distribution of

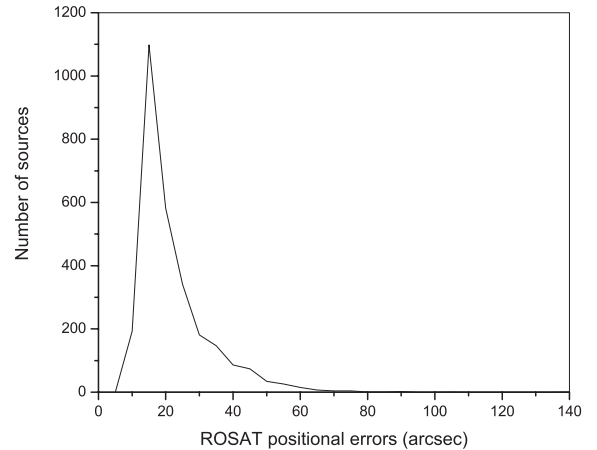


**Fig. 1.** Distribution of the ROSAT FSC positional errors for 2791 sources of interest.

positional errors ( $1\sigma$ ) for the 2791 ROSAT FSC sources to show the importance of discriminating between different error circles. Based on previous experience with identifications and knowledge of the physical nature of typical X-ray sources, we selected the most likely candidate counterpart among the objects in the error circle. In the case where two or more objects were likely, all were taken as counterparts to be checked later with additional information. As the HQS limiting magnitude is brighter than that of the DSS, the corresponding low-dispersion spectra were faint or even absent for a number of DSS objects. When there were no bright point-like objects in the error circle, the optical counterpart was typically a faint AGN rather than a faint star. We classified the faint optical counterpart then as an AGN given that the counterpart had a blue color and/or was extended. For the 95 ROSAT sources, we could not find any reliable counterpart. Most probably, their optical counterparts were fainter than the DSS limit.

For 2696 X-ray sources we found one or more plausible optical counterparts, altogether 3202 objects. Accurate DSS2 (red) positions were measured during the identification for all these objects, DSS2 (red) being the most accurate (Mickaelian 2004) and closest to the ROSAT observing epoch. Optical positions also allowed the optical-X-ray distances to be determined in units of the  $1\sigma$ -error radius, which gives a better estimate of the probability of correct identifications than do the absolute numbers. The simultaneous inspection of the HQS spectra and DSS1/DSS2 images allowed us to find a number of objects showing variability, extension, or proper motion.

Proper motions were found either among bright stars (including a number of late-type stars) or among white dwarfs (WD). In cases where the optical counterpart showing proper motion is faint, there is a high probability that it is a WD.

One of the most striking results is the possibility of a rough classification of objects not only from low-dispersion spectra, but also from DSS images alone. In cases where the object was blue as judged from comparing the DSS2 blue/red/IR images, we found a slight extension on the red and/or IR images for many of them. On the DSS2 blue image, the extension (the host galaxy) cannot be distinguished from the bright nucleus. The extension on the red and/or IR images is present almost

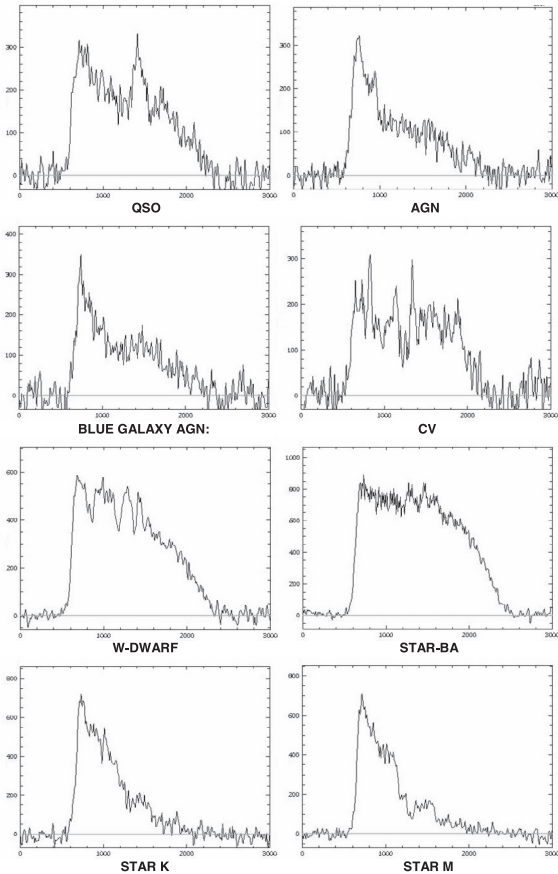


**Fig. 2.** Some sample HQS low-dispersion spectra for the main types of objects.

for all bright ( $<17.5^m$ ) AGN/QSOs with small redshifts. These objects are AGNs with high probability, as they have weak host galaxies and strong blue nuclei, and they are always found very close to the X-ray positions. Thus careful study of the three DSS2 images often leads to the identification of faint AGNs even without having low-dispersion spectra available.

### 3.2. The HQS classification criteria and object types

A description of the classification criteria based on HQS low-dispersion spectra has been given in the HRC papers (Bade et al. 1998; Zickgraf et al. 2003). Some sample spectra are shown in Fig. 2. The classification scheme adopted here might be called 2D, taking into account that the DSS direct images give information on the extension of the objects (most of the objects are point-like), and the HQS spectra give information on their spectral type. Therefore, in this case we separate AGNs into “QSOs” (point-like objects) and “AGNs” (extended objects). Compared to the HRC, there are fewer objects among our identifications classified as SATURATE, which correspond to very bright (typically  $B < 12^m$ ) objects. Using the 2D low-dispersion spectra on the spectral plates directly (together with the extracted 1D spectra used by the HRC), we could classify additional bright objects, which was not possible from the extracted 1D spectra alone. Moreover, examination of the 2D spectra allowed us to avoid artifacts and defects on the

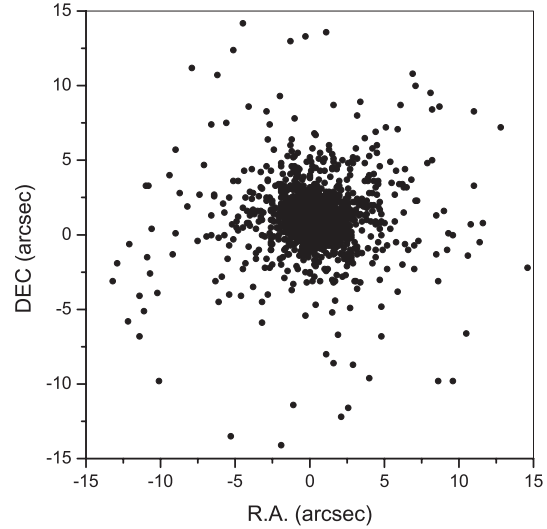


**Fig. 3.** The DSS2(red)-MAPS positional differences for 2341 objects in common.

spectra, which appear as features on 1D spectra. All faint objects classified as EBL-WK, BLUE-WK, and RED-WK, according to the classification criteria of the HRC (see Zickgraf et al. 2003), were reclassified here to known physical classes using all additional data that were available.

### 3.3. Cross-correlation with MAPS

After counterpart identification on the DSS and HQS plates we made a cross-correlation of the selected 3202 optical objects with the MAPS catalogue (Cabanela et al. 2003). We also checked the MAPS data for the ROSAT fields with no optical identification to see if there were very blue or very red objects, but without success. Our experience (Mickaelian et al. 2001) shows that this catalogue is rather good for homogeneous photometric data (magnitudes and colors). The separation of objects in MAPS into “stars” (point-like) and “galaxies” (extended) and application of two different measurement techniques (diameter-based, and integration of all pixels of the image, respectively) allows us to derive magnitudes with  $0.2^m$  accuracy, which is not the case for other catalogues (f.e. USNO-B1.0). MAPS gives  $O$  and  $E$  magnitudes measured from the POSS1 blue and red plates, respectively. Our accurate optical positions allowed a cross-correlation with a small search radius ( $3''$ ) helping to avoid a lot of close chance associations, which is one of the main problems for any cross-correlation. A number of proper motion objects, blends (rejected in MAPS), extended, bright (having inaccurate coordinates), or faint objects were not found in MAPS. For objects having proper motions, we repeated the search with positions measured on the DSS1 and found the corresponding MAPS objects. For extended and bright objects, we repeated the search with larger radii ( $10''$  and  $15''$ ) and have found them too. We show the DSS2(red)-MAPS positional differences in Fig. 3 for the associated objects, and 90% of associations are within  $3''$  radius.

We took the  $O$  magnitudes and the  $O - E$  colors for all objects found in MAPS as the optical photometric system used in the BHRC. In part, the photometry was used as a refinement of the classification. Using the MAPS classification into “stars” and “galaxies”, these associations also helped in a number of cases to distinguish between QSOs and WDs, when we were in doubt about the extension of the object.

### 3.4. Other available data

The next step was a search for associations in SIMBAD, NED, USNO-B1.0 (Monet et al. 2003), in catalogues of AGNs (Véron-Cetty & Véron 2003, hereafter VCV), WDs (McCook & Sion 2003), and cataclysmic variables (CVs, Ritter & Kolb 2003), and non-optical catalogues: NVSS (Condon et al. 1998), FIRST (Becker et al. 2003), IRAS (IRAS 1988; Moshir et al. 1990), and 2MASS (Cutri et al. 2003). There are relatively new versions of catalogues of AGNs, WDs, and CVs (all from 2003), which are more complete for these particular objects than the SIMBAD and NED data. All 3202 objects were checked in SIMBAD with search radii 10'', 30'', and 1' depending on brightness (bright objects more likely have uncertain positions in our DSS measurements, as well as in SIMBAD) and extension. There 996 optical objects and 195 non-optical (radio, IR, and other than ROSAT X-ray) sources were found, with radio sources pointing to plausible candidates for QSOs. All objects classified as any type of galaxy/AGN/QSO or as a doubtful star in SIMBAD (altogether 2143 objects) were checked in NED with a search radius of 1', and 1084 associations were found made up of 879 optical objects (QSOs, galaxies, groups, and clusters of galaxies) and 205 non-optical sources. A lot of objects had deviating classifications compared to those given in SIMBAD.

The USNO-B1.0 catalogue was used to search for proper motions (PM) and variability among a subsample of 583 objects. Included were the objects for which proper motions were found by comparing the DSS1 and DSS2 plates, suspected WDs, as well as all optically bright objects. According to the USNO-B1.0, 132 of these objects have proper motions  $\geq 30$  mas/yr. 21 of them with  $30 < PM < 80$  mas/yr were not among our list of PM candidates, since classified in part as QSO candidates. We therefore doubt the reliability of these USNO proper motions and conclude that a limit  $\approx 80$  mas/yr is required to obtain reliable proper motions from the USNO. We also found two objects with significant PM (150–300 mas/yr) but without PM listed in the USNO. Altogether, we have 113 objects with  $PM > 80$  mas/yr in the BHRC.

In addition, 156 variable objects were found in the USNO-B1.0 by comparing POSS1 with POSS2 magnitudes, including 5 known CVs and 3 flare stars. As the USNO photometry is not as reliable as the MAPS photometry, only objects showing magnitude differences  $> 0.5^m$  both in  $O$  and  $E$  were selected, and 35 of them show magnitude differences of  $> 1.0^m$  between POSS1 and POSS2.

Cross-correlations with the VCV, WD, and CV catalogues gave a number of new associations compared to the SIMBAD and NED data. There are 27 121 known QSOs/AGN in the

VCV catalogue in our area of interest. We found 322 associations in the 1' search radius, including 318 associations with our optical counterparts and 4 other (additional) objects. We checked the images of these 4 objects and found them rather faint (almost invisible even in the DSS2 blue). Most probably, they are chance associations, as we have reliable optical counterparts for all of the corresponding ROSAT sources. There are 1392 WDs in our area, but only 8 were found to be associated with our ROSAT sources. Out of 187 known CVs in our area, 7 were found to be associated with our ROSAT sources, including 1 object also found in the WD catalogue.

The total number of optical counterparts listed as optical detection already in at least one of the catalogues or databases is 1367. Most of them are (mainly bright) galaxies (539), (mainly bright) stars (406), QSOs (180), other AGNs (154), and systems of galaxies (42). Other objects are CVs (10), flare stars (10), WDs (8), and 18 of a miscellaneous nature.

For the remaining optical counterparts, we found 333 non-optical associations: 257 of them are radio (NVSS, FIRST, 87GB, etc.), 30 are IR (IRAS and 2MASS), and 46 are X-ray sources (detected by other X-ray missions than ROSAT). These non-optical associations helped with the final classification of the X-ray sources. For instance, many counterpart candidates were faint blue objects and could be identified either with QSOs or WDs. The association with a radio source helped to classify some of them as candidate QSO, rather than as WD.

In a final step we combined all information (including the ROSAT X-ray data) to select the most likely counterpart for each X-ray source.

## 4. Description of the catalogue

The Byurakan/Hamburg/ROSAT Catalogue (BHRC, Table 1) contains both the X-ray and optical data, including accurate ( $< 1$  arcsec) optical positions, magnitudes, colors, and object classifications. We should recall that most of our classifications mean candidates for these objects, as they were derived from the HQS low-dispersion spectra and/or DSS images. However, for those objects found to be known, we give the classifications given in the literature. Each entry in the BHRC corresponds to one optical counterpart. Thus, some ROSAT sources have more than one entry.

In case all counterparts are members of a group or a cluster, we make comments on this so that the user may consider all these objects together as one identification for the given source. Comments were also given on a number of X-ray counterparts for which another, possibly associated, object was found in the vicinity. These associated objects do not necessarily contribute to the X-ray emission. In the case where it is located within the  $3\sigma$  X-ray error radius, it is listed explicitly in the catalogue. Examples are objects with blue stellar spectra in the vicinity of AGN candidates, associations of galaxies, and stars in clusters.

The contents of the BHRC are as follows:

1. ROSAT name (1RXS Jhhmss.s+ddmss) (Voges et al. 2000);
2. ROSAT positional error (arcsec);
3. ROSAT count rate (photons/s);

4. ROSAT count rate error (photons/s);
5. ROSAT hardness ratio 1;
6. ROSAT hardness ratio 1 error;
7. ROSAT hardness ratio 2;
8. ROSAT hardness ratio 2 error;
9. optical counterpart component (for >1 counterparts);
10. DSS2 red J2000 RA (hh:mm:ss.ss);
11. DSS2 red J2000 Dec (dd:mm:ss.s);
12. distance between DSS2 red and X-ray position (arcsec);
13. distance between DSS2 red and X-ray position (as fraction of the ROSAT positional error);
14. MAPS  $O$  magnitude;
15. MAPS  $O - E$  color;
16. USNO-B1.0 proper motion (mas/yr);
17. USNO-B1.0  $O$  magnitude (mean of DSS1 blue and DSS2 blue);
18. USNO-B1.0  $E$  magnitude (mean of DSS1 red and DSS2 red);
19. USNO-B1.0  $O - E$  color (mean of DSS1  $O - E$  and DSS2  $O - E$ );
20. USNO-B1.0  $I$  magnitude (DSS2 IR);
21. USNO-B1.0 magnitude difference between DSS2 and DSS1 (mean of blue and red);
22. classification of the objects based on DSS images, HQS spectra, MAPS, and USNO-B1.0, SIMBAD/NED/AGN/WD/CV associations;
23. comments on the objects (binary and multiple stars; pairs, groups and clusters of galaxies and QSOs; variability, etc.);
24. associations with known optical objects from SIMBAD, NED, and AGN/WD/CV catalogues: types of objects;
25. optical associations: names of the objects;
26. optical associations: distance between the catalogue and DSS2 red (our) positions (arcsec);
27. optical associations: distance between the catalogue and ROSAT positions (arcsec);
28. optical associations: classification of objects;
29. optical associations: catalogue magnitudes (typically  $B$  magnitude);
30. optical associations: redshift;
31. associations with non-optical sources (radio, IR, other X-ray);
32. non-optical associations: names of the sources;
33. non-optical associations: distance between the source and DSS2 red (our) positions (arcsec);
34. non-optical associations: distance between the source and ROSAT positions (arcsec).

Table 2 shows selected columns from a section of the BHRC.

## 5. Discussion

### 5.1. Source statistics

The BHRC contains 3202 optical counterparts for 2696 X-ray sources. For 2248 X-ray sources a unique counterpart was found, while for 448 X-ray sources two or more optical counterparts may contribute to the X-ray emission. Of the 448 sources with multiple counterparts, 401 have two, 37 have

three, 9 have four, and 1 has five optical candidate counterparts. Thus in total, 954 optical counterparts are listed for the 448 X-ray sources.

In Table 3 the optical counterparts are listed according to their classification. The multiple counterparts are divided into subgroups U (“unique”) and A (“ambiguous”). The subgroup U comprises those sources for which all candidate counterparts belong to the same class of objects, for example a group or cluster of galaxies, and subgroup A all other multiple counterparts. The 364 counterparts of subgroup U belong to 144 X-ray sources, and in these cases an unambiguous identification can be assigned (see below). Subgroup A belongs to the remaining 304 X-ray sources with 590 optical counterpart candidates, in which the source of the X-ray emission is unclear. In these cases two or more highly probable counterparts (f.e. a QSO and a K-star) were found within the error radius.

#### 5.1.1. The AGN subsamples

The AGNs (QSO/BLL/AGN/Blue Galaxy) make up the largest group of counterparts comprising 58.1% (single counterparts) or 56.2% of all counterparts. They are easily found when having strong emission lines in the HQS spectra. Four strong emission lines, namely MgII, CIII, CIV, and Ly $\alpha$ , may appear in the HQS spectral range of 3400–5400 Å, in case the redshift is in the ranges 0.214–0.929 (MgII), 0.781–1.829 (CIII), 1.195–2.486 (CIV), and 1.796–3.441 (Ly $\alpha$ ). Depending on the line strength, we find these lines in HQS in 40–80% of cases.

Some high redshift QSOs have HQS spectra that are similar to faint late-type stars, and it is very difficult to recognize them only from the HQS. However, we have found that their colors are still blue when DSS2 blue/red/IR images (or MAPS and USNO catalogues) are compared. Thus additional information from the DSS is required to identify faint high redshift QSOs.

Altogether 215 AGN counterparts belong to U subgroup of multiple counterparts meaning that two or more blue counterparts were found in the error circle. Follow-up spectroscopy is needed to decide which counterpart is actually the AGN.

#### 5.1.2. The galaxy subsample

The remaining counterparts with extragalactic origins are bright galaxies, groups, and clusters of galaxies. The groups and clusters are contained mostly in subgroup U of Table 3. Among the pairs of galaxies, we find candidates for interacting/merging pairs, which are mostly of a red color compared to those of AGN candidates. For pairs, groups, and clusters of galaxies, the X-ray emission comes either from a dominating member or from the whole system. For a number of “bright galaxies”, ROSAT may have detected the integral X-ray emission, although the presence of an active nucleus cannot be excluded.

We show four examples for subgroup U multiple objects in Fig. 4: a galaxy group, a close galaxy group (“interacting group”), a close pair (“interacting pair”), and a “merger”, all unambiguous optical counterparts for the X-ray sources.

**Table 2.** A section of the Byurakan/Hamburg/ROSAT-FSC (BHRC) Catalogue of optical identifications of X-ray sources (only selected columns).

ROSAT source	Err "	CR ct/s	HR1	HR2	Comp	DSS2 RA h min s	DSS2 Dec d am as	opt-X "	$\sigma$	MAPS magO	MAPS color	Classification
1RXS J000008.1+295712	27	0.0410	-1.00	0.00		00 00 07.23	+29 57 01.0	15.8	0.6	14.62	-0.72	WD
1RXS J000023.9+265453	15	0.0463	-0.16	-0.08		00 00 24.13	+26 55 07.3	14.6	1.0	6.94	1.34	Star F
1RXS J000223.8+003059	27	0.0405	0.79	1.00		00 02 24.64	+00 32 06.5	68.7	2.5	19.62	1.87	AGN:
1RXS J000250.8+000824	26	0.0410	-0.32	0.09		00 02 51.59	+00 08 01.0	25.9	1.0	18.86	1.54	AGN
1RXS J000430.7+191335	14	0.0404	0.21	-0.01		00 04 30.81	+19 13 32.2	3.3	0.2	19.31	0.72	WD:
1RXS J000524.3+161934	15	0.0465	0.54	0.40		00 05 24.33	+16 19 46.1	12.1	0.8	9.23	1.26	Star G
1RXS J000546.7+020618	21	0.0588	-0.47	-0.78	a	00 05 46.70	+02 06 22.5	4.0	0.2			Galaxy blue
1RXS J000546.7+020618	21	0.0588	-0.47	-0.78	b	00 05 48.61	+02 06 31.1	31.2	1.5	20.46	3.02	Galaxy blue
1RXS J000600.8+111221	42	0.0417	0.79	0.08		00 06 02.16	+11 12 25.2	20.5	0.5	13.86	1.08	Star AF
1RXS J000611.4+145402	11	0.0417	0.78	0.37		00 06 11.54	+14 53 57.3	5.6	0.5	17.32	1.05	AGN:
1RXS J000624.4+105206	26	0.1090	1.00	0.70	a	00 06 20.31	+10 51 51.5	62.0	2.4	18.55	2.44	BLL
1RXS J000624.4+105206	26	0.1090	1.00	0.70	b	00 06 21.84	+10 51 01.2	75.0	2.9	15.90	1.69	Star K
1RXS J000648.1+250225	50	0.0735	0.41	-0.66		00 06 47.70	+25 01 43.8	41.6	0.8	20.17	1.07	AGN:
1RXS J000659.2+251950	31	0.0408	-0.05	-0.46		00 06 56.14	+25 19 48.2	41.5	1.3	21.81	2.63	Galaxy
1RXS J000716.0+263325	27	0.0448	0.91	0.47		00 07 15.13	+26 33 42.9	21.4	0.8	18.09	2.28	Galaxy
1RXS J000718.9+261717	12	0.0491	0.07	-0.51		00 07 19.09	+26 17 01.0	16.2	1.4	12.24	1.29	Star FG
1RXS J000730.4+061853	11	0.0474	0.79	0.56		00 07 29.32	+06 19 16.6	28.6	2.6	18.10	0.99	WD:
1RXS J000734.5+053704	16	0.0411	-0.57	0.16		00 07 34.85	+05 37 17.7	14.2	0.9	19.10	0.42	Galaxy blue
1RXS J000801.0+035501	17	0.0494	0.44	0.17		00 07 59.98	+03 55 10.4	17.9	1.1	18.83	0.49	QSO:
1RXS J000815.0+020240	25	0.0414	1.00	0.26		00 08 13.37	+02 02 17.1	33.4	1.3	17.45	0.70	Star K
1RXS J000859.0+255310	17	0.0447	0.76	0.34		00 08 59.28	+25 53 05.4	6.0	0.4	17.09	0.29	QSO
1RXS J000904.4+062828	11	0.0418	0.95	1.00		00 09 03.93	+06 28 21.0	10.2	0.9	21.42	1.62	AGN
1RXS J000915.3+055805	14	0.0439	0.79	0.22		00 09 15.26	+05 58 16.4	11.4	0.8	20.71	0.93	QSO:
1RXS J000919.2+173216	17	0.0534	-0.90	-0.25		00 09 19.55	+17 32 04.7	12.4	0.7	7.88	2.22	Star G
1RXS J000929.3+122252	11	0.0480	0.21	-0.04		00 09 29.54	+12 22 50.8	3.7	0.3	10.20	1.12	Star F
1RXS J001000.1+134336	20	0.0501	0.91	0.11		00 09 59.43	+13 43 34.2	10.0	0.5	16.73	0.76	AGN:
1RXS J001015.9+174643	18	0.0416	0.22	0.58		00 10 17.74	+17 47 29.1	52.6	2.9	19.05	2.78	Star M:
1RXS J001027.3+105826	10	0.1170	0.76	0.56		00 10 27.52	+10 58 47.7	22.0	2.2	19.02	1.10	AGN:
1RXS J001029.4+204743	13	0.0428	0.92	0.06		00 10 28.74	+20 47 49.8	11.1	0.9	18.75	0.71	QSO
1RXS J001030.3+105609	26	0.0433	1.00	0.38		00 10 33.32	+10 55 59.5	45.5	1.8	20.21	0.49	Galaxy blue

### 5.1.3. The stellar subsample

The stellar counterparts are mostly relatively bright stars ( $12^m$ – $13^m$ ) of spectral type F-G and late-type stars of spectral type K and M (“coronal emitters”). The “bright stars” listed have  $m < 12^m$  and have no spectral classification because of saturation on the HQS plates. Several dozen white dwarf and cataclysmic variable candidates were found, which are usually optically fainter.

### 5.2. Reliability and efficiency of the identification strategy

A few tests were made to access the reliability and the efficiency of the identification strategy.

### 5.2.1. Comparison with the HRC

In Table 4 we compare our classification statistics with those of the HRC. For this purpose our classifications were combined to match the HRC classifications as closely as possible. The table shows that the identifications for BSC and FSC X-ray sources are rather similar, except for the increase in the fraction of AGNs in the BHRC, which is due to additional faint counterparts found on the DSS images.

If we add the “unidentified” and “no spectrum” objects in the HRC to the QSO/AGN category, we obtain 56.4%, which almost exactly corresponds to the QSO/AGN fraction in the BHRC. All other classes of objects have similar shares among the identifications, except the F-G and K stars. However, the total stellar fraction is similar ( $\sim 30$ – $33\%$ ), so that the spectral type assignments have to be different between HRC and BHRC. Probably the missing F-G and K stars in the HRC

**Table 3.** The statistics of the optical counterparts in the BHRC catalogue by classification. For the definition of the subgroups of multiple counterparts, see text.

Classification	Single	Multiple		Total	%
		U	A		
Bright galaxy	27	0	6	33	1.0
Galaxy	130	74	54	258	8.1
QSO	858	172	138	1168	36.5
BLL	11	0	5	16	0.5
AGN	334	25	83	442	13.8
Blue galaxy	103	18	54	175	5.5
HII region	2	0	0	2	0.1
Planet. Neb.	1	0	0	1	0.0
White dwarf	26	2	4	32	1.0
CV	12	0	0	12	0.4
Bright star	11	0	8	19	0.6
Stars B-A	52	2	20	74	2.3
Stars F-G	429	41	100	570	17.8
Star K	201	30	92	323	10.1
Star M	46	0	23	69	2.2
Star C	1	0	1	2	0.1
Star:	4	0	2	6	0.2
All objects	2248	364	590	3202	100.0

have to be searched for among the “bright stars”, which have saturated HQS spectra. In the BHRC, many bright stars were classified from already existing catalogues or on the base of the unsaturated parts of the 2D HQS spectra.

To check the efficiency of the identification technique and the use of additional data, we conducted an identification of 104 ROSAT BSC sources with no identification in the HRC. We could find counterparts for 101 of them (97%). It appears that most of them are faint QSO candidates that are not present on the HQS plates and therefore missed in the HRC. This result agrees with the suggestion that the missing fraction of AGN counterparts in the HRC compared to the BHRC (Table 4) is hidden among the unidentified sources in the HRC.

### 5.2.2. Comparison with the VCV catalogue

To estimate the reliability of our initial classification based on the HQS low-dispersion spectra and the DSS direct images, we compared them with the 305 objects in common with the VCV catalogue. We should reiterate that many counterpart candidates show blue spectra in HQS and no other features. These might be QSOs, WDs, CVs, or just main-sequence early-type stars. But, as the stellar types are rather rare as X-ray counterparts, these objects are in fact mostly QSOs.

We found only 11 objects that have not been classified as AGN (4%), which means that counterparts displaying QSO/AGN properties as seen in the low-dispersion spectra really turn out to be genuine QSO/AGN.

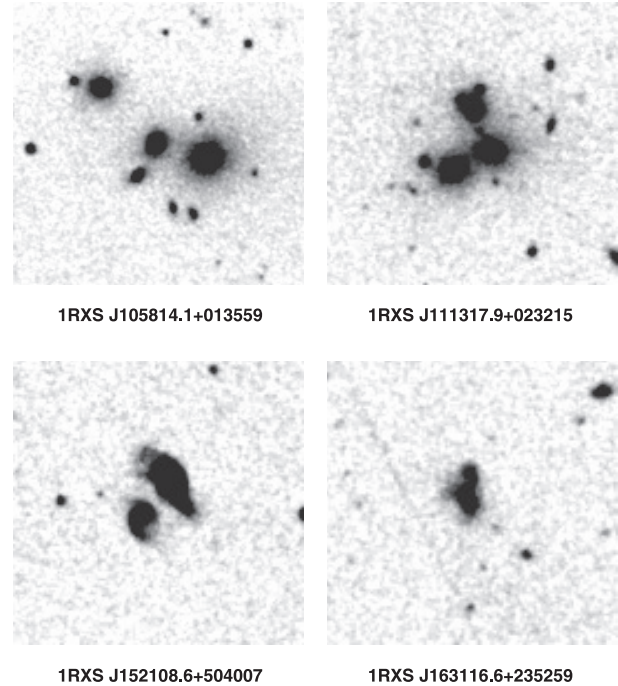


**Fig. 4.** Examples of multiple objects being unambiguous optical counterparts: a galaxy group (*top left*), a close galaxy group (*top right*), a close galaxy pair (*bottom left*), and a “merger” (*bottom right*).

**Table 4.** Comparison of the HRC and BHRC classifications.

Class	HRC		BHRC	
	number	%	number	%
blank field	155	2.9	95	3.4
galaxy	238	4.5	140	4.4
galaxy cluster	262	4.9	153	4.8
QSO/AGN	2215	41.5	1801	56.2
white dwarf	45	0.8	33	1.0
CV	26	0.5	12	0.4
bright stars	1219	22.8	93	2.9
F-G star	45	0.8	570	17.8
K star	141	2.6	323	10.1
M star / C star	197	3.7	71	2.2
unidentified	604	11.3	6	0.2
no spectrum	194	3.6	–	–
All sources	5341	100.0	2791	100.0
All counterparts	5341	100.0	3202	100.0

Note: galaxy clusters include multiple galaxies and groups; bright stars include stars that have been classified as B-A types.

## 5.3. General properties of the counterparts

### 5.3.1. Positional accuracy

In Fig. 5 we give the distribution of optical-X-ray positional distances in fractions of the X-ray error radius. About 65% of the counterparts are located within the  $1\sigma$  error radius. Only a few objects appear to be located outside of  $3\sigma$ , but these are

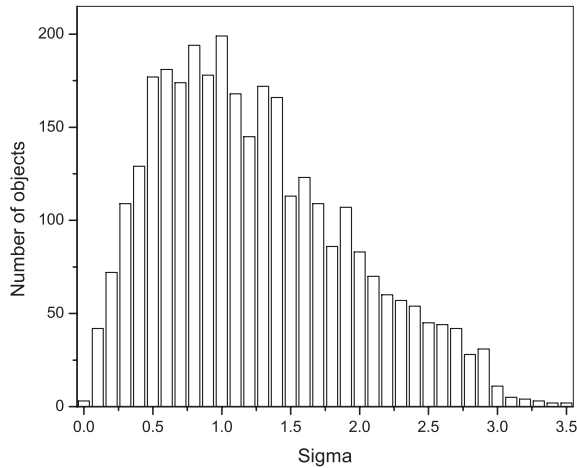


**Fig. 5.** The DSS2(red)-ROSAT positional differences for 3202 selected optical counterparts in fractions of the ROSAT error radius.

components of multiple counterparts (stars or galaxies) identified with a single X-ray source.

### 5.3.2. Optical magnitudes and colors

The cross-correlation with the MAPS catalogue allowed us to obtain homogeneous optical magnitudes and colors for the counterparts. In Fig. 6 we plot MAPS  $O - E$  colors against  $O$ -magnitude. The point-like objects form two distinct groups; a genuine star sequence (F-G-K-M sequence from left to right with increasing color indices) and a region occupied by QSOs (between 16th and 21th magnitudes and with colors between  $-1.0$  and  $+1.5$ ).

In Fig. 7 we show the distributions of MAPS  $O$  magnitudes for point-like objects (QSOs/AGN, WDs, and other stars) and extended objects (galaxies). Point-like counterparts have a first maximum at  $12^m - 13^m$ , which is made up of the bright part of the stellar sequence in Fig. 6, while the second maximum is dominated by the QSOs/AGN. Galaxies identified as counterparts are typically faint with  $O > 17$  mag.

## 6. Summary

We present the Byurakan/Hamburg/ROSAT Catalogue of optical identifications for 2791 northern high-galactic latitude X-ray sources. The catalogue contains 65.4% of extragalactic sources and 34.6% of stellar emitters. The majority of the extragalactic sources,  $\sim 86\%$ , are AGN (QSOs, BLL, Sy). Stellar sources are mostly main-sequence stars with spectral types F-G-K-M. A small number of sources are WDs and CVs, and only  $\sim 3\%$  of sources remain unidentified. The source statistics of the BHRC containing ROSAT X-ray sources with count rates between  $0.04$  and  $\approx 0.05 \text{ s}^{-1}$  is in good agreement with that of the HRC containing the brighter X-ray sources from the ROSAT All-Sky Survey. The only difference is a higher fraction of identified AGN candidates due to the detection of fainter counterparts in the DSS images.

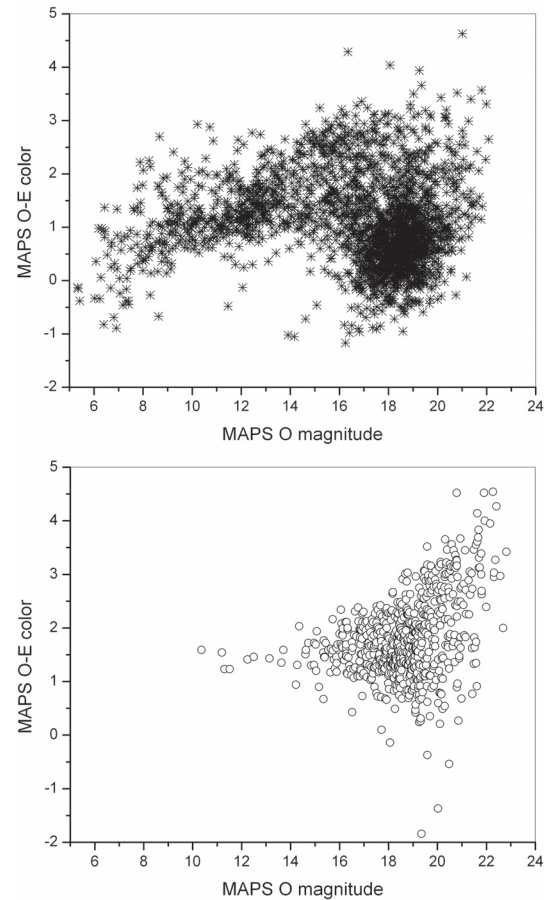


**Fig. 6.** MAPS color–magnitude diagram for point-like objects (*top*) and galaxies (*bottom*).

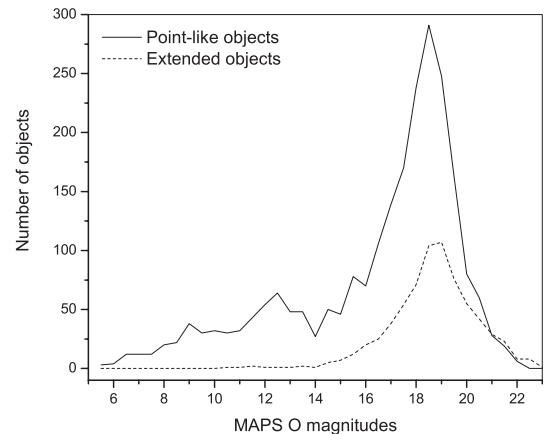


**Fig. 7.** Distribution of the MAPS  $O$  magnitudes for point-like objects and galaxies.

The BHRC can be used as a database for the selection of different samples of soft X-ray emitters for detailed follow-up studies, as well as for studies of particular objects.

*Acknowledgements.* The authors are grateful to F.-J. Zickgraf for the use of his identification software and for useful discussions and comments on the paper.

We are thankful to the referee Dr. M. P. Véron for her careful reading of the manuscript and a number of comments, which improved the paper.



The ROSAT project was supported by the Bundesministerium für Bildung und Wissenschaft and the Max-Planck-Gesellschaft.

The Hamburg Quasar Survey (HQS) was supported by the Deutsche Forschungsgemeinschaft through grants Re 353/11-1, 2, 3 and Re 353/22-1, 2, 3.

The Digitized Sky Surveys were produced at the Space Telescope Science Institute under U.S. Government grant NAG W-2166. The images of these surveys are based on photographic data obtained using the Oschin Schmidt Telescope on Palomar Mountain and the UK Schmidt Telescope. The plates were processed into the present compressed digital form with the permission of these institutions. The National Geographic Society – Palomar Observatory Sky Atlas (POSS-I) was made by the California Institute of Technology with grants from the National Geographic Society.

The Second Palomar Observatory Sky Survey (POSS-II) was made by the California Institute of Technology with funds from the National Science Foundation, the National Geographic Society, the Sloan Foundation, the Samuel Oschin Foundation, and the Eastman Kodak Corporation. The Oschin Schmidt Telescope is operated by the California Institute of Technology and Palomar Observatory.

The MAPS catalogue is supported by the National Science Foundation, the National Aeronautics and Space Administration, and the University of Minnesota, and is available at <http://aps.umn.edu/>.

## References

- Appenzeller, I., Thiering, I., Zickgraf, F.-J., et al. 1998, *ApJS*, 117, 319
- Bade, N., Engels, D., Voges, W., et al. 1998, *A&AS*, 127, 145
- Becker, R. H., Helfand, D. J., White, R. L., et al. 1997, The FIRST Survey Catalog, Version 2003 Apr. 11, *ApJ*, 475, 479
- Cabanela, J. E., Humphreys, R. M., Aldering, G., et al. 2003, *PASP*, 115, 837
- Condon, J. J., Cotton, W. D., Greisen, E. W., et al. 1998, *AJ*, 115, 1693
- Cotton, B. 1999, at [www.cv.nrao.edu/bcotton/fitsview.html](http://www.cv.nrao.edu/bcotton/fitsview.html)
- Cutri, R. M., Skrutskie, M. F., Van Dyk, S., et al. 2003, The 2MASS All-Sky Catalog. Final Release, Univ. Mass. and IPAC/CalTech
- Fischer, J.-U., Hasinger, G., Schwobe, A. D., et al. 1998, *AN*, 319, 347
- Hagen, H.-J., Groote, D., Engels, D., & Reimers, D. 1995, *A&AS*, 111, 195
- Henry, J. P., Gioia, I. M., Mullis, C. R., et al. 2001, *ApJ*, 553, 109
- IRAS 1988, Joint IRAS Science Working Group. Infrared Astronomical Satellite Catalogs, The Point Source Catalog, Version 2.0, NASA RP-1190
- Krautter, J., Zickgraf, F.-J., Appenzeller, I., et al. 1999, *A&A*, 350, 743
- Lasker, B. M., Doggett, J., McLean, B., et al. 1996, *ASP Conf. Ser.*, 101, 88
- McCook, G. P., & Sion, E. M. 1999, *ApJS*, 121, 1 (Version June 2003 in CDS, Catalog No. III/235)
- McGlynn, T., White, N. E., & Scollick, K. 1994, *ASP Conf. Ser.*, 61, 34
- Mickaelian, A. M. 2004, *A&A*, 426, 367
- Mickaelian, A. M., Gonçalves, A. C., Véron-Cetty, M. P., & Véron, P. 2001, *Ap*, 44, 14
- Monet, D., Bird, A., Canzian, B., et al. 1996, The USNO-A2.0 Catalogue (Washington DC: U.S. Naval Observatory)
- Monet, D. G., Levine, S. E., Casian, B., et al. 2003, The USNO-B1.0 Catalogue, *AJ*, 125, 984
- Moshir, M., Kopan, G., Conrow, T., et al. 1990, Infrared Astronomical Satellite Catalogs, The Faint Source Catalog, Version 2.0, NASA
- Ritter, H., & Kolb, U. 2003, *A&A*, 404, 301
- Schmidt, M., & Green, R. F. 1983, *ApJ*, 269, 352
- Schwobe, A., Hasinger, G., Lehmann, I., et al. 2000, *AN*, 321, 1
- Trümper, J. 1983, *Adv. Space Res.*, 2, 4, 241
- Véron-Cetty, M.-P., & Véron, P. 2003, *A&A*, 412, 399
- Véron-Cetty, M.-P., Balayan, S. K., Mickaelian, A. M., et al. 2004, *A&A*, 414, 487
- Voges, W., Aschenbach, B., Boller, Th., et al. 1999, *A&A*, 349, 389
- Voges, W., Aschenbach, B., Boller, Th., et al. 2000, *IAU Circ.*, 7432
- Voges, W., Henry, J. P., Briel, U. G., et al. 2001, *ApJ*, 553, 119
- Zickgraf, F.-J., Thiering, I., Krautter, J., et al. 1997, *A&AS*, 123, 103
- Zickgraf, F.-J., Engels, D., Hagen, H.-J., et al. 2003, *A&A*, 406, 535